Original Article | Neuroimaging and Head & Neck

eISSN 2005-8330
https://doi.org/10.3348/kjr.2018.0685
Korean J Radiol 2019;20(4):662-670

Korean Journal of Radiology
KJR

Relationship between Abnormal Hyperintensity on T2-Weighted Images Around Developmental Venous Anomalies and Magnetic Susceptibility of Their Collecting Veins: *In-Vivo* Quantitative Susceptibility Mapping Study

Yangsean Choi, MD, Jinhee Jang, MD, Yoonho Nam, PhD, Na-Young Shin, MD, Hyun Seok Choi, MD, So-Lyung Jung, MD, Kook-Jin Ahn, MD, Bum-soo Kim, MD

All authors: Department of Radiology, Seoul St. Mary's Hospital, College of Medicine, The Catholic University of Korea, Seoul, Korea

Objective: A developmental venous anomaly (DVA) is a vascular malformation of ambiguous clinical significance. We aimed to quantify the susceptibility of draining veins (χ_{vein}) in DVA and determine its significance with respect to oxygen metabolism using quantitative susceptibility mapping (QSM).

Materials and Methods: Brain magnetic resonance imaging of 27 consecutive patients with incidentally detected DVAs were retrospectively reviewed. Based on the presence of abnormal hyperintensity on T2-weighted images (T2WI) in the brain parenchyma adjacent to DVA, the patients were grouped into edema (E+, n = 9) and non-edema (E-, n = 18) groups. A 3T MR scanner was used to obtain fully flow-compensated gradient echo images for susceptibility-weighted imaging with source images used for QSM processing. The χ_{vein} was measured semi-automatically using QSM. The normalized χ_{vein} was also estimated. Clinical and MR measurements were compared between the E+ and E- groups using Student's t-test or Mann-Whitney U test. Correlations between the χ_{vein} and area of hyperintensity on T2WI and between χ_{vein} and diameter of the collecting veins were assessed. The correlation coefficient was also calculated using normalized veins.

Results: The DVAs of the E+ group had significantly higher χ_{vein} (196.5 ± 27.9 vs. 167.7 ± 33.6, $p = 0.036$) and larger diameter of the draining veins ($p = 0.006$), and patients were older ($p = 0.006$) than those in the E- group. The χ_{vein} was also linearly correlated with the hyperintense area on T2WI ($r = 0.633$, 95% confidence interval 0.333–0.817, $p < 0.001$).

Conclusion: DVAs with abnormal hyperintensity on T2WI have higher susceptibility values for draining veins, indicating an increased oxygen extraction fraction that might be associated with venous congestion.

Keywords: *Developmental venous anomaly; Quantitative susceptibility mapping; Vascular malformation; Magnetic resonance imaging*

INTRODUCTION

Developmental venous anomaly (DVA) is a common vascular malformation with an estimated incidence of 2.5% (1). It is referred to as "caput medusae" because of multiple fine veins draining into a single collecting vein of unusual location and size (2). While imaging and clinical findings suggest DVAs to be an embryologic variant of venous

Received October 3, 2018; accepted after revision December 31, 2018.
This study was supported by Basic Science Research Program through the National Research Foundation of Korea (NRF) funded by the Ministry of Education (NRF-2017R1D1A1B03033829).

Corresponding author: Jinhee Jang, MD, Department of Radiology, Seoul St. Mary's Hospital, College of Medicine, The Catholic University of Korea, 222 Banpo-daero, Seocho-gu, Seoul 06591, Korea.
• Tel: (822) 2258-5799 • Fax: (822) 599-6771 • E-mail: znee@catholic.ac.kr

Korean Journal of Radiology
KJR

drainage, its clinical significance remains controversial (3). Occasionally, brain parenchyma with DVA exhibits abnormal T2 hyperintensity (4, 5), and a recent study suggested that this hyperintensity is associated with venous congestion (6). Manifestation of venous congestion in other similar vascular malformations, such as dural arteriovenous fistula (dAVF), is important as it necessitates careful decisions in treatment strategies (7, 8). The increased risk of hemorrhagic complications associated with DVAs has been previously reported when they coexist with arteriovenous fistula (9). Similarly, another report suggested that DVAs with T2 hyperintensity are prone to hemorrhagic complications (5). Hence, detailed characterization of DVAs with abnormal hyperintensity on T2-weighted images (T2WI) might help to understand the clinical significance of DVAs.

Venous congestion affects the oxygen metabolism of related brain parenchyma (10). Differences in oxygen metabolism might have varying clinical significance in several neurovascular diseases (8, 11, 12). A study using positron emission tomography (8) showed that symptomatic dAVF had decreased cerebral blood flow, venous congestion, and increased oxygen extraction fraction (OEF); symptoms and abnormal oxygen metabolism were found to be resolved after treatment of dAVF. The clinical importance of increased OEF was also discovered as an independent predictor of future ischemic stroke in patients with cerebral and carotid arterial occlusion (11, 12). Although assessing the metabolic characteristics of DVA might help to understand its clinical significance, few studies have explored changes in oxygen metabolism in DVA in association with venous congestion.

Phase magnetic resonance (MR) images allow good contrast differentiation between diamagnetic oxyhemoglobin and paramagnetic deoxyhemoglobin (13), and are thus capable of demonstrating details of vascular structures and their oxygenation status. A few studies have shown that phase MR images can help characterize DVA with venous congestion (1, 5, 14). However, these studies visually assessed unwrapped phase images or susceptibility-weighted images (SWI) of DVA. To better understand the effect of venous congestion on DVA, it would be more desirable to quantify the effect of oxygen metabolism in a specific region of the brain. Recently, a method was proposed to quantitatively estimate the oxygenation status of a structure of interest using phase information from MR images and the quantitative susceptibility mapping (QSM) measurement (15, 16). In this study, we applied QSM to assess the association between venous congestion and oxygen metabolism of DVA. The purpose of this study was to explore the value of QSM in quantifying oxygen metabolism in DVA with abnormal hyperintensity on T2WI and compare clinical and QSM characteristics of DVA with and without T2 hyperintensity.

MATERIALS AND METHODS

Study Population

This retrospective study was approved by the Institutional Review Board, which waived the requirement for informed consent. From January 2015 to June 2017, we identified 132 DVAs showing typical MR findings using the Picture Archiving and Communication System database. Exclusion criteria were 1) other coincidental brain lesions, such as cavernous malformation, posing as potential artifacts for QSM (n = 50); 2) different MR scanners (n = 26); 3) different MR scan protocols, such as omission of three-dimensional (3D) gradient echo (GRE) images for QSM (n = 23); 4) suboptimal location of DVA for QSM analysis (i.e., too close to the skull base) (n = 2); and 5) a diameter of the collecting vein of the DVA smaller than 0.5 mm for appropriate analysis (n = 4). Finally, 27 patients with DVA meeting the criteria made up the final study population. Patient demographics and symptoms for magnetic resonance imaging (MRI) studies were collected through a review of medical records. Clinical indications for MR imaging were 1) follow-up imaging for aneurysm (n = 1) and epilepsy (n = 2); 2) workup for neuropsychiatric diseases (n = 3); 3) dizziness (n = 4); 4) headaches (n = 8); 5) memory impairment (n = 2); 6) evaluation of brain metastasis (n = 3); 7) pre-operative workup (n = 2); and 8) traumatic brain injury (n = 2).

MR Imaging and QSM Processing

MR images were obtained from a 3T MRI unit (MAGNETOM Verio; Siemens Healthineers Sector, Erlangen, Germany) with a 12-channel coil. Fully flow-compensated GRE images were obtained for SWI, and the source images were used for QSM processing. Acquisition parameters were as follows: TR = 28 ms, TE = 20 ms, FA = 15°, FOV = 230 x 172.5 mm, matrix size = 320 x 240, and slice thickness = 2 mm. Axial T2WI of the brain were obtained with vendor-specific standard protocols. Contrast-enhanced axial T1-weighted images (T1WI) were obtained according to the clinical circumstances.

QSM was automatically generated from the GRE magnitude

 https://doi.org/10.3348/kjr.2018.0685

and phase images (Fig. 1). First, phase unwrapping was performed for the phase image of each echo time using a Laplacian-based unwrapping algorithm (17). Before QSM calculation, brain masking was performed using the Brain Extraction Tool (18) in the FMRIB Software Library Ver 5.0 (FMRIB, Oxford, UK). The background frequency (mainly induced from outside the brain) was removed through harmonic phase removal using the Laplacian operator (HARPERELLA) method (19). QSM was calculated using the improved sparse linear equation and least-squares method (20). As cusp artifacts in phase images (21) or an incorrectly generated brain mask could cause severe errors in the QSM calculation process, an MR physicist carefully examined the images for these errors before we proceeded to the region of interest (ROI) analysis. All processes of parametric mapping were performed using MATLAB (R2016a; MathWorks Inc., Natick, MA, USA).

MR Image Assessment

Two radiologists evaluated the T2WI (with or without fluid-attenuated inversion recovery preparation) in consensus to detect hyperintensity associated with DVA. These images were compared with other images, such as contrast-enhanced T1WI, to clearly localize the DVAs. The reviewers visually assessed the presence of T2 hyperintensity compared with adjacent brain parenchyma and divided the patients into two groups: DVA with abnormal hyperintensity on T2WI (edema group; E+) and DVA without it (non-edema group; E-). For the E+ DVA group, the area of hyperintensity on T2WI was measured with a semi-automatically drawn ROI using a region-growing algorithm (Insight Segmentation and Registration Toolkit connected threshold image filter) (22) and measurements were made in consensus. If T2 hyperintensity was found in more than one slice of the MR images, ROIs were drawn for each slice, and a summation of these areas was acquired.

QSM Image Analysis for the Collecting Veins of DVA

We measured the susceptibility value of the collecting veins on QSM to estimate the oxygen metabolism status of brain parenchyma draining via DVA. To measure susceptibility values of thin collecting veins accurately and reliably, we implemented a semi-automatic method to extract susceptibility values. Instead of manually placing a tiny ROI on the thin collecting veins, two radiologists drew an oval ROI > 25 mm^2 on the QSM images in consensus that covered the collecting vein and surrounding brain parenchyma (Fig. 2). T2WI and QSM images were compared side-by-side to exclude hyperintense parenchyma in the ROI. Based on the susceptibility of normal white matter and venous structures (23-25), a threshold of 100 ppb was used to divide draining veins and adjacent brain parenchyma (26, 27). Clear demarcation of collecting veins and surrounding brain parenchyma was achieved when using this threshold (Fig. 2). Mean susceptibility of voxels over the threshold (100 ppb) was used to estimate the susceptibility of draining vein (χ_{vein}). Mean values of the remaining voxels were used to estimate the susceptibility of the adjacent brain tissue ($\chi_{background}$). To minimize the effect of a local variation of susceptibility to venous structures, normalized

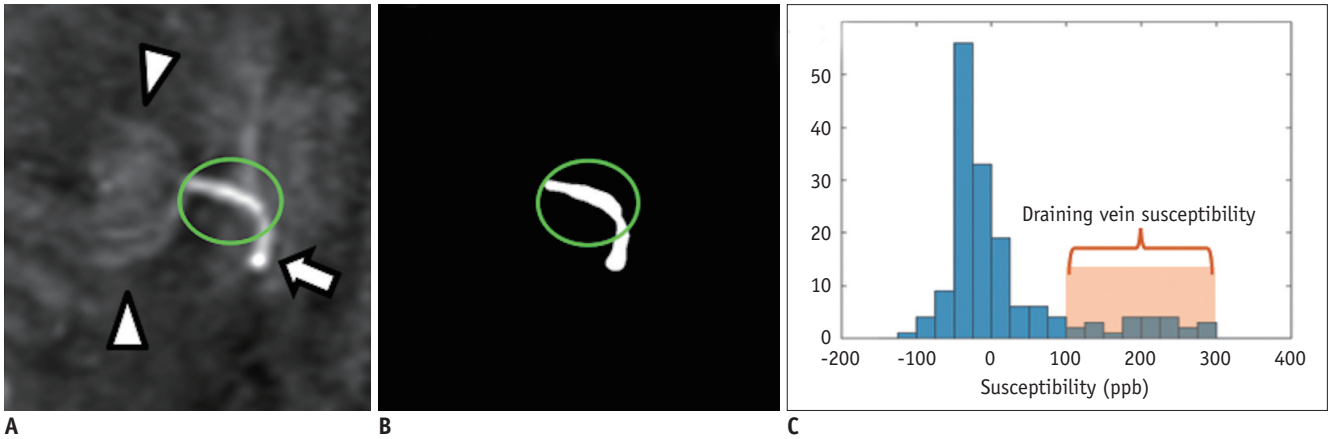

Fig. 1. Susceptibility measurement of collecting vein of DVA.
A. ROI was drawn on QSM image for collecting vein (arrow), but not on DVA itself (arrowheads). **B.** Note clear demarcation of draining vein at threshold of 100 ppb. **C.** On histogram of ROI-voxel susceptibility values, mean susceptibility of voxels over threshold (100 ppb) was used to estimate susceptibility of draining vein. Mean value of remaining voxels was used to measure susceptibility of adjacent brain tissue. DVA = developmental venous anomaly, QSM = quantitative susceptibility mapping, ROI = region of interest

https://doi.org/10.3348/kjr.2018.0685

Korean Journal of Radiology
KJR

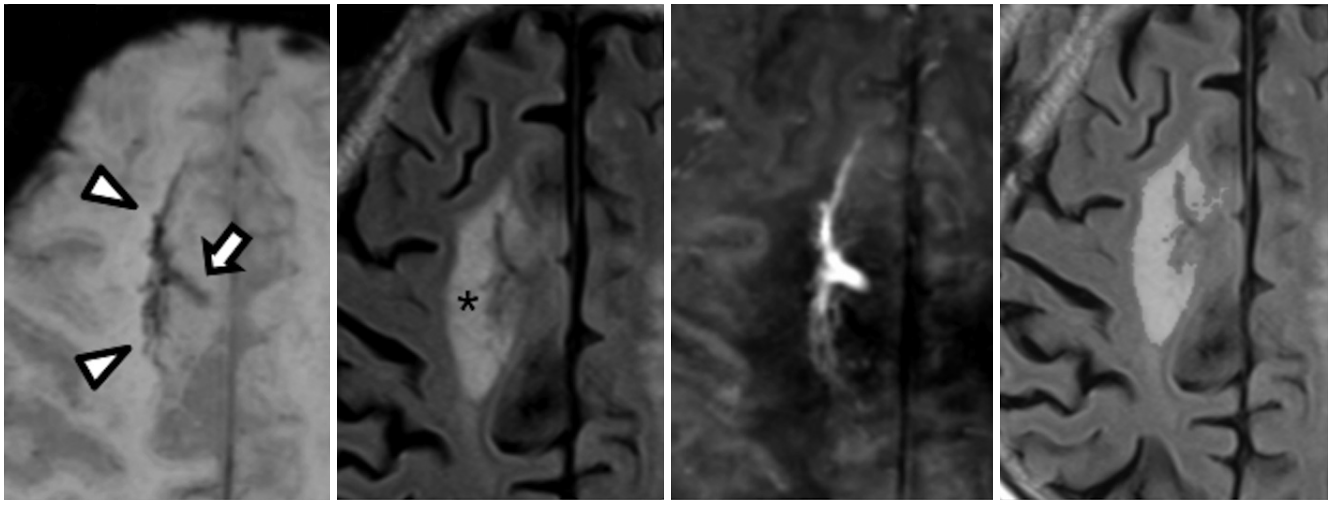

Fig. 2. 86-year-old female with DVA in right frontal lobe.
SWI **(A)** shows DVA itself (arrowheads) and collecting vein (arrow). T2-weighted fluid-attenuated inversion recovery image **(B)** shows large area of T2 hyperintensity (asterisk). On QSM image **(C)**, paramagnetic venous structure of DVA is well demonstrated. χ_{vein} is 233 ppb and normalized χ_{vein} is 238 ppb. Diameter of collecting vein is 2.7 mm and T2 hyperintensity area is 9.63 mm^2 **(D)**. SWI = susceptibility weighted images, χ_{vein} = susceptibility of draining veins

Table 1. Patient Characteristics

Characteristics	DVA with T2 Hyperintensity (Group E+; n = 9)	DVA without T2 Hyperintensity (Group E-; n = 18)	*P*
Sex (M/F)	5/4	10/8	1
Age (years)	66.9 ± 14.3	45.2 ± 19.3	0.006
DVA location			
Frontal lobe	7	8	
Parietal lobe	1	3	
Temporal	1	2	
Cerebellum	0	5	
Edema area (cm^2)	4.7 ± 4.4	0.0 ± 0.0	0.012
Diameter of collecting veins (mm)	2.1 ± 0.4	1.8 ± 0.7	0.349

DVA = developmental venous anomaly

susceptibility values of the collecting veins were obtained (normalized $\chi_{vein} = \chi_{vein} - \chi_{background}$). To verify the QSM process, we drew another ROI on the normal contralateral brain parenchyma to measure the susceptibility value of control brain parenchyma ($\chi_{control}$).

Diameters of collecting veins were measured on T2WI in conjunction with 3D contrast-enhanced T1WI for accurate analysis. In doing so, blooming artifacts of the venous structure noted on SWI, as well as partial volume artifacts on 2D images, were avoided. Diameters of collecting veins were measured at the mid-portion of the straightest segment, approximately 10 mm distal to the convergence of the draining veins.

Statistical Analysis

Clinical and MR measurements of DVAs were compared between E+ and E- groups using Student's *t* test or Mann-Whitney U test. In addition, correlations between the χ_{vein} and area of T2 hyperintensity, and between the χ_{vein} and diameter of collecting veins were assessed. The correlation coefficient was also calculated using the normalized χ_{vein}. All analyses were performed with R (version 3.2.4, R Foundation, Vienna, Austria; www.r-project.org) statistical packages.

RESULTS

Among 27 DVAs, nine DVAs showed abnormal T2 hyperintensity (E+ group) in the draining area and the

https://doi.org/10.3348/kjr.2018.0685

other 18 showed no parenchymal signal changes (E- group) on T2WI (Table 1). E+ patients (age, mean ± standard deviation, 66.9 ± 14.3 years) were significantly older than E- patients (45.2 ± 19.3 years, $p = 0.006$). Twenty-two DVAs were in the supratentorial and five were in the infratentorial area. No DVA was found in the occipital lobe. Mean area of T2 hyperintensity in the E+ group was 4.7 ± 4.4 cm^2. The diameter of collecting veins was not significantly different between the two groups ($p = 0.349$). Representative cases are presented in Figures 2 and 3.

The χ_{vein} of the E+ group (196.5 ± 27.9 ppb) (Table 2) was significantly higher than that of the E- group (167.7 ± 33.6 ppb, $p = 0.036$), suggesting a higher concentration of deoxyhemoglobin within the collecting veins. The normalized χ_{vein} was also significantly higher in the E+ group (202.0 ± 32.6 ppb) than in the E- group (163.6 ± 32.3 ppb, $p = 0.007$). However, the $\chi_{background}$ and $\chi_{control}$ were not significantly different between the two groups (Table 2). The χ_{vein} ($r = 0.633$, 95% confidence interval [CI] 0.333–0.817, $p < 0.001$) (Fig. 4A) was positively correlated with the diameter of collecting veins. Additionally, χ_{vein} showed a significant positive correlation with the area of T2 hyperintensity ($r = 0.444$, 95% CI 0.076–0.705, $p = 0.020$) (Fig. 4B).

DISCUSSION

In this study, we found a significant association between the presence of venous congestion and oxygen metabolism in DVA. This suggests that QSM might be used to characterize DVA from a metabolic perspective. Although DVA is thought to be clinically benign, neurologic symptoms and complications of DVA have been reported (1, 3-5, 9, 14, 28). A previous study by Takasugi et al. (5) suggested the possible clinical significance of T2 hyperintensity associated with DVA, by theorizing that abnormal T2 hyperintensity might be associated with venous congestion and increased risk of complications. As DVAs are functional adaptations to the absence of normal venous pathways (3, 28), they might not be able to provide sufficient venous drainage (29) and

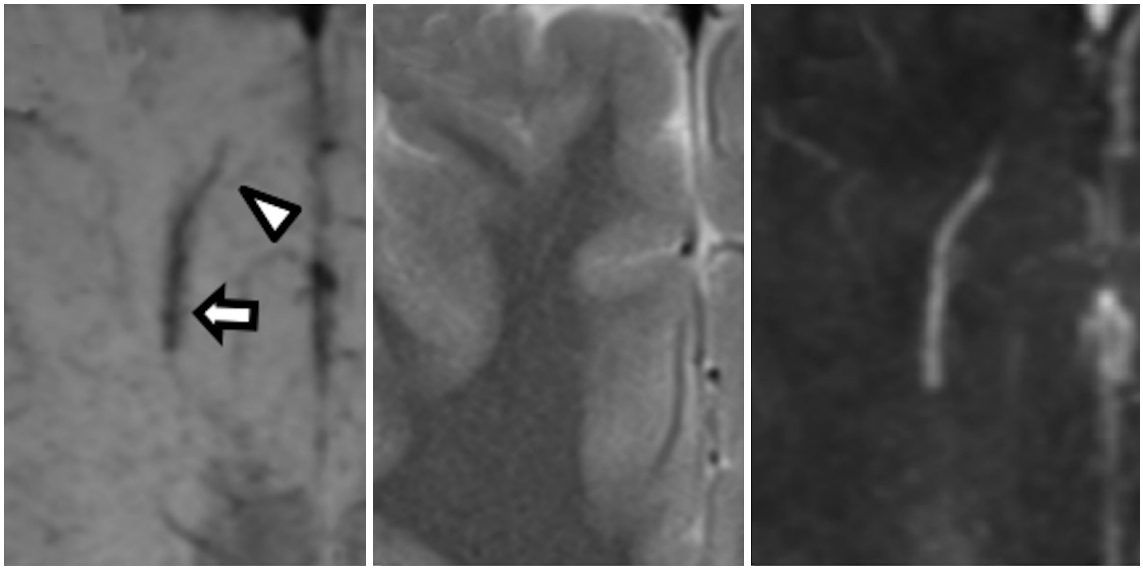

Fig. 3. 36-year-old male with DVA in his right frontal lobe.
SWI **(A)** shows DVA itself (arrowhead) and collecting vein (arrow). On T2-weighted image **(B)**, no hyperintensity is observed. On QSM image **(C)**, χ_{vein} is 142 ppb and normalized χ_{vein} is 145 ppb with diameter of 1.04 mm.

Table 2. Susceptibility Values for Collecting Veins and Other Brain Areas

Susceptibility	DVA with T2 Hyperintensity (Group E+; n = 9)	DVA without T2 Hyperintensity (Group E-; n = 18)	*P*
χ_{vein} (ppb)	196.5 ± 27.9	167.7 ± 33.6	0.036
$\chi_{background}$ (ppb)	-5.6 ± 12.0	4.1 ± 15.9	0.122
Normalized χ_{vein} (ppb)	202.0 ± 32.6	163.6 ± 32.3	0.007
$\chi_{control}$ (ppb)	-7.8 ± 27.7	-14.8 ± 11.2	0.459

χ_{vein} = susceptibility of draining veins, $\chi_{background}$ = susceptibility of adjacent brain tissue, $\chi_{control}$ = susceptibility value of control brain parenchyma

https://doi.org/10.3348/kjr.2018.0685

Korean Journal of Radiology
KJR

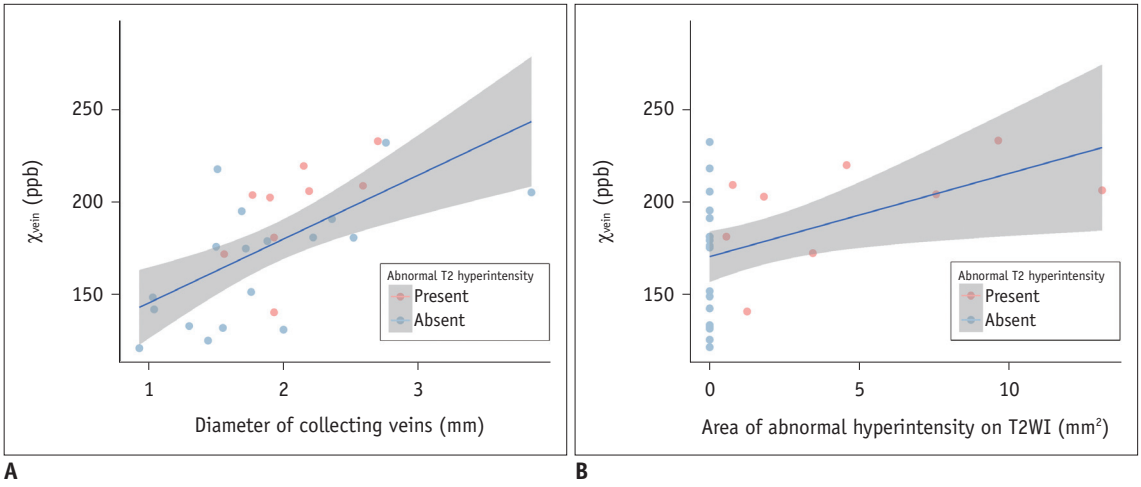

Fig. 4. Scatter plots demonstrating relationship between χ_{vein} with respect to (A) diameter of collecting veins and (B) area of abnormal hyperintensity on T2-weighted image with moderate positive correlations (A: $r = 0.633$, $p < 0.001$, B: $r = 0.444$, $p = 0.020$). Regression lines are drawn in blue and their 95% confidence intervals are shown as grey areas. T2WI = T2-weighted images

thus, might be prone to venous congestion. In addition to venous congestion, concomitant altered oxygen metabolism might be associated with the neurological manifestation of DVA and related complications (5, 14, 28), as in other neurovascular diseases (8, 11, 12). Considering these previous observations, we thought that the relatively large variability of oxygen metabolism in DVA-associated brain areas may explain the clinical characteristics of DVA.

In DVAs with venous congestion, χ_{vein} was significantly higher than those without congestion. The high χ_{vein} of DVA with venous congestion suggests high concentrations of deoxyhemoglobin (15) and OEF. With venous congestion, OEF can be increased due to prolonged transit time via capillary beds (6). The range of susceptibility of veins in the E+ and E- groups was comparable with results from a previous study on acute ischemic stroke where the susceptibility of ischemic territories was higher than that of healthy control regions (254 ± 48 and 125 ± 8 ppb, respectively) (30). We postulated that the modified oxygen metabolism of DVA with abnormal T2 hyperintensity would have a similar microvascular environment to that of ischemic lesions. We also found a positive correlation between the χ_{vein} and the area of T2 hyperintensity. A larger T2 hyperintense area suggested more venous congestion in terms of extent and severity, and more increased OEF. Similar findings were observed in dAVF on SWI (7, 31); other studies found that SWI demonstrated prominent hypointensity of veins in dAVF, which was associated with symptoms and venous congestion (31, 32). On positron emission tomography, abnormal perfusion and elevated OEF were observed in dAVF with venous congestion, and these abnormalities were reversed after treatment (8).

DVAs of the E+ group had larger collecting vein diameters compared with DVAs of the E- group. Furthermore, the collecting vein diameter was significantly negatively correlated with the χ_{vein}. One possible explanation is that the DVA might have a smaller venous functional capacity than that of normal venous structures. Due to the embryonic background of DVAs (3, 28), they might show insufficient draining function, especially for large brain areas. DVAs responsible for large brain areas might be more likely to have "insufficient venous drainage" despite the large caliber of the collecting veins. Another possible explanation is that veins with congestion are more likely to be dilated than are those without congestion (31). Interestingly, no T2 hyperintensity was observed among the five cerebellar DVAs (Table 1), a finding consistent with a previous similar study (4); differences in parenchymal area between cerebral and cerebellar hemispheres–and the corresponding supra- and infratentorial venous drainage–might be responsible for such a phenomenon. Additionally, patients in the E+ group were older than patients in the E- group, raising the possibility that this change could be a chronic course of failure of adaptation. Increased OEF might also be associated with chronic venous congestion and insufficiency (11, 12).

Previous studies used phase MR images to assess the characteristics of DVA, such as venous congestion (5, 14). However, these studies only performed visual inspection of phase MR images or SWI. They did not quantify phase

 https://doi.org/10.3348/kjr.2018.0685

or susceptibility values of DVA, and their methods did not allow quantitative investigation of the association between venous congestion and regional oxygen metabolism. We used QSM instead, which resolved the non-localized effect and orientation dependency of the susceptibility source (24). We could quantify the susceptibility values more precisely, the results of which would probably have greater clinical value compared with qualitative image findings alone.

Several recent studies have explored the clinical value of oxygen metabolism in the brain (15, 33). To estimate regional oxygen metabolism, it is crucial to define specific venous structures that receive the venous drainage of the brain area in question (15). However, due to multiple draining channels and anatomical venous variations in the brain, it is challenging to correlate specific regional draining veins to specific regions of the brain. For example, in vascular malformations, defining the main draining vein is very difficult due to the complex vascular architecture and multiple drainage routes. However, in DVAs, we can easily define the draining vein because a single collecting vein is present. By assessing the susceptibility value of the collecting vein, we can easily estimate the oxygen metabolism of the brain parenchyma, which drains via DVA.

There were some limitations of this study. Because of its retrospective nature, some unexpected biases, including selection bias, might have been introduced. However, we reviewed a relatively large number of consecutive patients and included patients after a thorough review. The relatively small number of subjects limited the detailed analysis of the association of venous congestion and morphological characteristics of the DVA, such as venous kinking of the collecting veins. Furthermore, we excluded patients who were imaged using different MR scanners or MR protocols, especially those with images that were not fully flow-compensated. A relatively large number of cavernous malformation cases were excluded since the malformation induces prominent streak artifacts from strongly paramagnetic sources, limiting local susceptibility estimation (34). Second, we defined the presence of venous congestion using abnormal hyperintensity on T2WI, rather than using perfusion- or diffusion-weighted images. As this process was not included in our routine MR protocol, we reviewed the conventional imaging findings instead. Future studies comparing abnormalities between perfusion, diffusion, and vasogenic edema to the χ_{vein} on DVA are needed. Third, we did not estimate the regional OEF or cerebral oxygen metabolism ratio since estimating them required additional clinical data such as arterial oxygen saturation or hematocrit levels and cerebral perfusion measures. Instead, the χ_{vein} was used to directly estimate the oxygenation status of the collecting veins. In addition, we normalized the χ_{vein} to correct for individual and local variability in the susceptibility estimation. Lastly, we could not correlate the patients' symptoms with abnormal T2 hyperintensity or the χ_{vein}. Any possible causal relationship between them was ambiguous due to the incidental and asymptomatic nature of DVAs. As a result, routine clinical and imaging follow-up of these patients was not warranted, limiting the extent of possibly useful information regarding the clinical course of DVAs with abnormal T2 hyperintensity.

In conclusion, DVA with venous congestion manifesting as abnormal hyperintensity on T2WI might be associated with different oxygen metabolisms in the brain parenchyma. 3D GRE and QSM imaging might be useful tools in the characterization of DVA with abnormal T2 hyperintensity with respect to oxygen metabolism.

Conflicts of Interest

The authors have no potential conflicts of interest to disclose.

ORCID iDs

Jinhee Jang
https://orcid.org/0000-0002-3386-1208
Yangsean Choi
https://orcid.org/0000-0003-1674-7101
Yoonho Nam
https://orcid.org/0000-0003-2149-0072
Na-Young Shin
https://orcid.org/0000-0003-1157-6366
Hyun Seok Choi
https://orcid.org/0000-0003-4999-8513
So Lyung Jung
https://orcid.org/0000-0002-3267-8399
Kook-Jin Ahn
https://orcid.org/0000-0001-6081-7360
Bum-soo Kim
https://orcid.org/0000-0002-3870-6813

REFERENCES

1. Amemiya S, Aoki S, Takao H. Venous congestion associated with developmental venous anomaly: findings on susceptibility weighted imaging. *J Magn Reson Imaging*

https://doi.org/10.3348/kjr.2018.0685

2008;28:1506-1509
2. Saba PR. The caput medusae sign. *Radiology* 1998;207:599-600
3. Rammos SK, Maina R, Lanzino G. Developmental venous anomalies: current concepts and implications for management. *Neurosurgery* 2009;65:20-29; discussion 29-30
4. San Millan Ruiz D, Delavelle J, Yilmaz H, Gailloud P, Piovan E, Bertramello A, et al. Parenchymal abnormalities associated with developmental venous anomalies. *Neuroradiology* 2007;49:987-995
5. Takasugi M, Fujii S, Shinohara Y, Kaminou T, Watanabe T, Ogawa T. Parenchymal hypointense foci associated with developmental venous anomalies: evaluation by phase-sensitive MR imaging at 3T. *AJNR Am J Neuroradiol* 2013;34:1940-1944
6. Jung HN, Kim ST, Cha J, Kim HJ, Byun HS, Jeon P, et al. Diffusion and perfusion MRI findings of the signal-intensity abnormalities of brain associated with developmental venous anomaly. *AJNR Am J Neuroradiol* 2014;35:1539-1542
7. Signorelli F, Gory B, Maduri R, Guyotat J, Pelissou-Guyotat I, Chirchiglia D, et al. Intracranial dural arteriovenous fistulas: a review of their current management based on emerging knowledge. *J Neurosurg Sci* 2017;61:193-206
8. Iwama T, Hashimoto N, Takagi Y, Tanaka M, Yamamoto S, Nishi S, et al. Hemodynamic and metabolic disturbances in patients with intracranial dural arteriovenous fistulas: positron emission tomography evaluation before and after treatment. *J Neurosurg* 1997;86:806-811
9. Roh JE, Cha SH, Lee SY, Jeon MH, Cho BS, Kang MH, et al. Atypical developmental venous anomaly associated with single arteriovenous fistula and intracerebral hemorrhage: a case demonstrated by superselective angiography. *Korean J Radiol* 2012;13:107-110
10. Wehrli FW, Rodgers ZB, Jain V, Langham MC, Li C, Licht DJ, et al. Time-resolved MRI oximetry for quantifying CMRO(2) and vascular reactivity. *Acad Radiol* 2014;21:207-214
11. Yamauchi H, Fukuyama H, Nagahama Y, Nabatame H, Ueno M, Nishizawa S, et al. Significance of increased oxygen extraction fraction in five-year prognosis of major cerebral arterial occlusive diseases. *J Nucl Med* 1999;40:1992-1998
12. Grubb RL, Jr., Derdeyn CP, Fritsch SM, Carpenter DA, Yundt KD, Videen TO, et al. Importance of hemodynamic factors in the prognosis of symptomatic carotid occlusion. *JAMA* 1998;280:1055-1060
13. Liu C, Li W, Tong KA, Yeom KW, Kuzminski S. Susceptibility-weighted imaging and quantitative susceptibility mapping in the brain. *J Magn Reson Imaging* 2015;42:23-41
14. Fushimi Y, Miki Y, Togashi K, Kikuta K, Hashimoto N, Fukuyama H. A developmental venous anomaly presenting atypical findings on susceptibility-weighted imaging. *AJNR Am J Neuroradiol* 2008;29:E56
15. Wehrli FW, Fan AP, Rodgers ZB, Englund EK, Langham MC. Susceptibility-based time-resolved whole-organ and regional tissue oximetry. *NMR Biomed* 2017;30. doi: 10.1002/nbm.3495. Epub 2016 Feb 26
16. Zhang J, Liu T, Gupta A, Spincemaille P, Nguyen TD, Wang Y. Quantitative mapping of cerebral metabolic rate of oxygen ($CMRO_2$) using quantitative susceptibility mapping (QSM). *Magn Reson Med* 2015;74:945-952
17. Schofield MA, Zhu Y. Fast phase unwrapping algorithm for interferometric applications. *Opt Lett* 2003;28:1194-1196
18. Smith SM. Fast robust automated brain extraction. *Hum Brain Mapp* 2002;17:143-155
19. Joshi NV, Vesey AT, Williams MC, Shah AS, Calvert PA, Craighead FH, et al. ^{18}F-fluoride positron emission tomography for identification of ruptured and high-risk coronary atherosclerotic plaques: a prospective clinical trial. *Lancet* 2014;383:705-713
20. Li W, Wang N, Yu F, Han H, Cao W, Romero R, et al. A method for estimating and removing streaking artifacts in quantitative susceptibility mapping. *Neuroimage* 2015;108:111-122
21. Haacke EM, Liu S, Buch S, Zheng W, Wu D, Ye Y. Quantitative susceptibility mapping: current status and future directions. *Magn Reson Imaging* 2015;33:1-25
22. Yoo TS, Ackerman MJ, Lorensen WE, Schroeder W, Chalana V, Aylward S, et al. Engineering and algorithm design for an image processing Api: a technical report on ITK--the insight toolkit. *Stud Health Technol Inform* 2002;85:586-592
23. Bilgic B, Pfefferbaum A, Rohlfing T, Sullivan EV, Adalsteinsson E. MRI estimates of brain iron concentration in normal aging using quantitative susceptibility mapping. *Neuroimage* 2012;59:2625-2635
24. Langkammer C, Schweser F, Krebs N, Deistung A, Goessler W, Scheurer E, et al. Quantitative susceptibility mapping (QSM) as a means to measure brain iron? A post mortem validation study. *Neuroimage* 2012;62:1593-1599
25. Deistung A, Schafer A, Schweser F, Biedermann U, Turner R, Reichenbach JR. Toward in vivo histology: a comparison of quantitative susceptibility mapping (QSM) with magnitude-, phase-, and R2*-imaging at ultra-high magnetic field strength. *Neuroimage* 2013;65:299-314
26. Chai C, Guo R, Zuo C, Fan L, Liu S, Qian T, et al. Decreased susceptibility of major veins in mild traumatic brain injury is correlated with post-concussive symptoms: a quantitative susceptibility mapping study. *Neuroimage Clin* 2017;15:625-632
27. Liu J, Xia S, Hanks R, Wiseman N, Peng C, Zhou S, et al. Susceptibility weighted imaging and mapping of micro-hemorrhages and major deep veins after traumatic brain injury. *J Neurotrauma* 2016;33:10-21
28. Taoka T, Fukusumi A, Miyasaka T, Kawai H, Nakane T, Kichikawa K, et al. Structure of the medullary veins of the cerebral hemisphere and related disorders. *Radiographics* 2017;37:281-297
29. Truwit CL. Venous angioma of the brain: history, significance, and imaging findings. *AJR Am J Roentgenol* 1992;159:1299-1307
30. Xia S, Utriainen D, Tang J, Kou Z, Zheng G, Wang X, et al. Decreased oxygen saturation in asymmetrically prominent cortical veins in patients with cerebral ischemic stroke. *Magn*

Reson Imaging 2014;32:1272-1276
31. Letourneau-Guillon L, Krings T. Simultaneous arteriovenous shunting and venous congestion identification in dural arteriovenous fistulas using susceptibility-weighted imaging: initial experience. *AJNR Am J Neuroradiol* 2012;33:301-307
32. Nakagawa I, Taoka T, Wada T, Nakagawa H, Sakamoto M, Kichikawa K, et al. The use of susceptibility-weighted imaging as an indicator of retrograde leptomeningeal venous drainage and venous congestion with dural arteriovenous fistula: diagnosis and follow-up after treatment. *Neurosurgery* 2013;72:47-54; discussion 55
33. Liu Z, Li Y. Cortical cerebral blood flow, oxygen extraction fraction, and metabolic rate in patients with middle cerebral artery stenosis or acute stroke. *AJNR Am J Neuroradiol* 2016;37:607-614
34. Shmueli K, de Zwart JA, van Gelderen P, Li TQ, Dodd SJ, Duyn JH. Magnetic susceptibility mapping of brain tissue in vivo using MRI phase data. *Magn Reson Med* 2009;62:1510-1522

https://doi.org/10.3348/kjr.2018.0685